Renewable and Sustainable Energy Reviews 15 (2011) 3676–3689

Contents lists available at ScienceDirect

Renewable and Sustainable Energy Reviews

journal homepage: www.elsevier.com/locate/rser

The potential of PEM fuel cell for a new drinking water source

Taeyoung Kim [a,b], Seungjae Lee [a], Heekyung Park [a,*]

[a] Department of Civil and Environmental Engineering, KAIST, Guseong-dong, Yuseong-gu, Daejeon, Republic of Korea
[b] Fuel Cell Research Center, Korea Institute of Energy Research, 102, Gajeong-ro, Yuseong-gu, Daejeon, Republic of Korea

ARTICLE INFO

Article history:
Received 21 December 2010
Accepted 24 June 2011
Available online 6 August 2011

Keywords:
PEM fuel cell
Drinking water source
Air stoichiometry
Air pressure
Cell temperature

ABSTRACT

The worldwide water scarcity, especially in the developing countries and arid regions, forces people to rely on unsafe sources of drinking water. There is a pressing need for these regions to develop decentralized, small-scale water utilities. However, more than 50% of the total operating costs associated with such small-scale, water-utility operations are the cost of providing electricity to run water pumps. We think that advances in a variety of renewable and sustainable energy technologies offer considerable promise for reducing the energy required for the production and distribution of water by small-scale water utilities. This paper provides a comprehensive review of the potential for using proton exchange membrane (PEM) fuel cells to provide an alternative supply of drinking water. This system can eliminate the excessive energy requirements that are currently associated with water production. Such alternative water production processes are designed to increase the production rate of drinking water by reducing the amount of water required to humidify the reactant gases during stable cell performance. The principal operational components of PEM fuel cells are reviewed and evaluated, including air stoichiometry, pressure, and cell temperature. Hydrogen-fed fuel cell systems provide sufficient water to meet the potable water needs of a typical household. Furthermore, it is concluded that PEM fuel cells have great promise for decentralized, small-scale, water-production applications, because they are capable of generating sufficient quantities of potable water by operating at maximum power and by increasing the number of polymer membranes.

Contents

1. Introduction

Water is an essential resource that is required for life and good health. Yet, 33% of the people in the world do not have enough water to meet their daily needs. Globally, the problem is getting worse as the population increases, which results in increases in the need for water in households and industries. When potable water is scarce, people are forced to rely on unsafe sources of drinking water. Poor water quality can increase the risk of diarrhoeal diseases, such as cholera, typhoid fever, and dysentery, which are the second leading cause of death in children under five years old. Impure water can also cause many other water-borne infections that are life-threatening. One quarter of the global population lives in developing countries that face water shortages due to the lack of

* Corresponding author. Tel.: +82 42 350 3620; fax: +82 42 350 3610.
E-mail address: hpark57@kaist.edu (H. Park).

1364-0321/$ – see front matter © 2011 Elsevier Ltd. All rights reserved.
doi:10.1016/j.rser.2011.06.006

Nomenclature

a	capture efficiency of effluent water in condenser (%)
A	total membrane area (cm^2)
EW	equivalent weight of polymer membrane
F	Faraday constant (96,485 C mol^{-1})
i	current density (A cm^{-2})
I	current (A)
MEA	membrane electrode assembly
$m_{a,d}$	mass of dry hydrogen at anode inlet (kg s^{-1})
$m_{c,d}$	mass of dry air at cathode inlet (kg s^{-1})
$m_{a,w}$	mass of water present in anode inlet (kg s^{-1})
$m_{c,w}$	mass of water present in cathode inlet (kg s^{-1})
m_{H_2O}	molecular mass of water (18.02 g mol^{-1})
M_C	amount of captured water at condenser per day (kg d^{-1})
M_D	amount of available drinking water per day (kg d^{-1})
M_H	water amount supplied for internal humidification per day (kg d^{-1})
M_P	amount of water production through electrochemical reaction (kg d^{-1})
p_a	total pressure at anode inlet (atm)
p_c	total pressure at cathode inlet (atm)
$p_{a,w,in}$	water partial pressure at anode inlet (atm)
$p_{c,w,in}$	water partial pressure at cathode inlet (atm)
$p_{a,w,out}$	water partial pressure at anode outlet (atm)
$p_{c,w,out}$	water partial pressure at cathode outlet (atm)
p^{sat}	saturated water vapor pressure of inlet gas (atm)
p^{sat}_{cell}	saturated water vapor pressure at given cell temperature (atm)
$RH_{a,in}$	hydrogen relative humidity at anode inlet (%)
$RH_{c,in}$	air relative humidity at cathode inlet (%)
$RH_{a,out}$	hydrogen relative humidity at anode outlet (%)
$RH_{c,out}$	air inlet relative humidity at cathode outlet (%)
T_1	entry temperature of the air at compressor (K)
x_{H_2O}	mole fraction of water vapor in the exhaust air gas

Greek symbols

α	net water drag coefficient (mol s^{-1} cm^{-2})
λ_c	air stoichiometry number
λ_a	hydrogen stoichiometry number
η_c	compressor efficiency
η_m	efficiency of the electric drive for the compressor

infrastructure that acquire water from rivers and aquifers. Water scarcity occurs even in areas where there is plenty of rainfall or freshwater. In arid and semi-arid regions, where water scarcity is more serious and endemic by definition, groundwater has played a major role in meeting domestic and irrigation demands. Groundwater mining and the lack of adequate planning have opened a new debate within legal frameworks and governance on the sustainability of the intensive use of groundwater. Desalination systems are also a viable alternative for solving the water shortage. However, conventional desalination systems are usually large-scale systems, which are more suitable for energy-rich and economically advanced regions. Also, they cause environmental degradation because they are fossil-fuel driven and because of the problem of brine disposal [1].

Furthermore, we are not fully aware of the linkages between energy, water, and sanitation service. In general, the electricity usage to convey, treat, and distribute water for all uses amounts to more than 20% of the total electricity usage in the United States [2]. Quite often, more than 50% of the total operating costs associated with small-scale water utility operations are the cost of the electricity required to run the water pumps. Furthermore, unreliable power supply results in increased energy costs due to the need for back-up power and for installation of protection systems to prevent damage to electrical systems. Inefficiency in the operation of water utilities results in high levels of non-revenue-producing water and unaccounted for water. The use of old equipment that is past its operational lifespan results in higher energy costs and inefficiency in system operations. The lack of energy-efficient system designs increases the operational and maintenance costs for the utilities, and their operational costs are increased further by damage to the electrical installations in water supply and sanitation systems caused by an unreliable power supply. Thus, we think that advances in a variety of renewable and sustainable energy technologies offer considerable promise for reducing the energy required for the production and distribution of water by small-scale water utility companies. In particular, hydrogen-fed fuel cells generate pure water, electricity, and heat energy through electrochemical reactions. Among the hydrogen-fed fuel cells, the proton exchange membrane (PEM) fuel cells are widely used due to high power density, quick response to changes in current demand, low operating temperature, and relatively low cost. Hristovski et al. [3] indicated that PEM fuel cells, as electrical energy and safe water production systems, could make a significant contribution to the future hydrogen economy. If appropriate renewable energy technologies, such as wind and solar, are designed for stable hydrogen supply, the fuel cell systems will eliminate the hundreds of miles of pipelines required to convey water from sensitive aquatic ecosystems. Furthermore, they may be advantageous for inland regions where water distribution is uneven. In the following sections, PEM fuel cell systems are introduced as viable water production systems, and useful guidelines for suitable ranges of operational parameters are provided to increase the amount of drinking water generated by PEM fuel cells.

2. Production of drinking water from fuel cell

The Gemini spacecraft was the first to use an alkaline electrolyte fuel cell to provide electricity as well as drinking water for the astronauts [4]. In an alkaline electrolyte fuel cell, hydroxyl ions (OH^-) are mobile, and, as they approach the anode, they react with hydrogen, releasing electrons; then, water is produced at the anode as a byproduct through electrochemical reaction. However, problems are encountered in the use of water generated by fuel cells, because the water contains sulfobenzoic acid, *p*-benzaldehyde sulfonic acid, and formaldehyde due to the degradation of the organic electrode [5]. Even though the water can be treated by means of filtration, carbon sorption, and ion exchange resins, none of these methods has proven to be sufficiently effective to make safe, potable water. These problems were resolved in the Apollo program by replacing the organic electrodes with sintered nickel electrodes, which do not degrade. Consequently, the fuel cell systems aboard the Apollo spacecraft produced safe water of extremely high quality at a peak rate of 1 kg h^{-1}. In 1998, Orta et al. [6] conducted a study of the quality of water generated by fuel cells aboard the U.S. Space Shuttle and the Russian Mir Space Station. According to their analytical results, the water generated aboard both spacecraft was high quality, with only a few anions and cations at μg/L concentrations. In 2009, Hristovski et al. [3] examined the quality of the water generated by various PEM fuel cells with different external humidification systems. Water samples were collected from six different PEM fuel cell systems, and their constituents were measured. The quality of the water generated by fuel cells was directly related to the quality of the input water supplied from different external humidification systems. However, the quality parameters of the water generated by PEM fuel cells were below the maximum contaminant levels with the exception of zinc, lead, and antimony, which

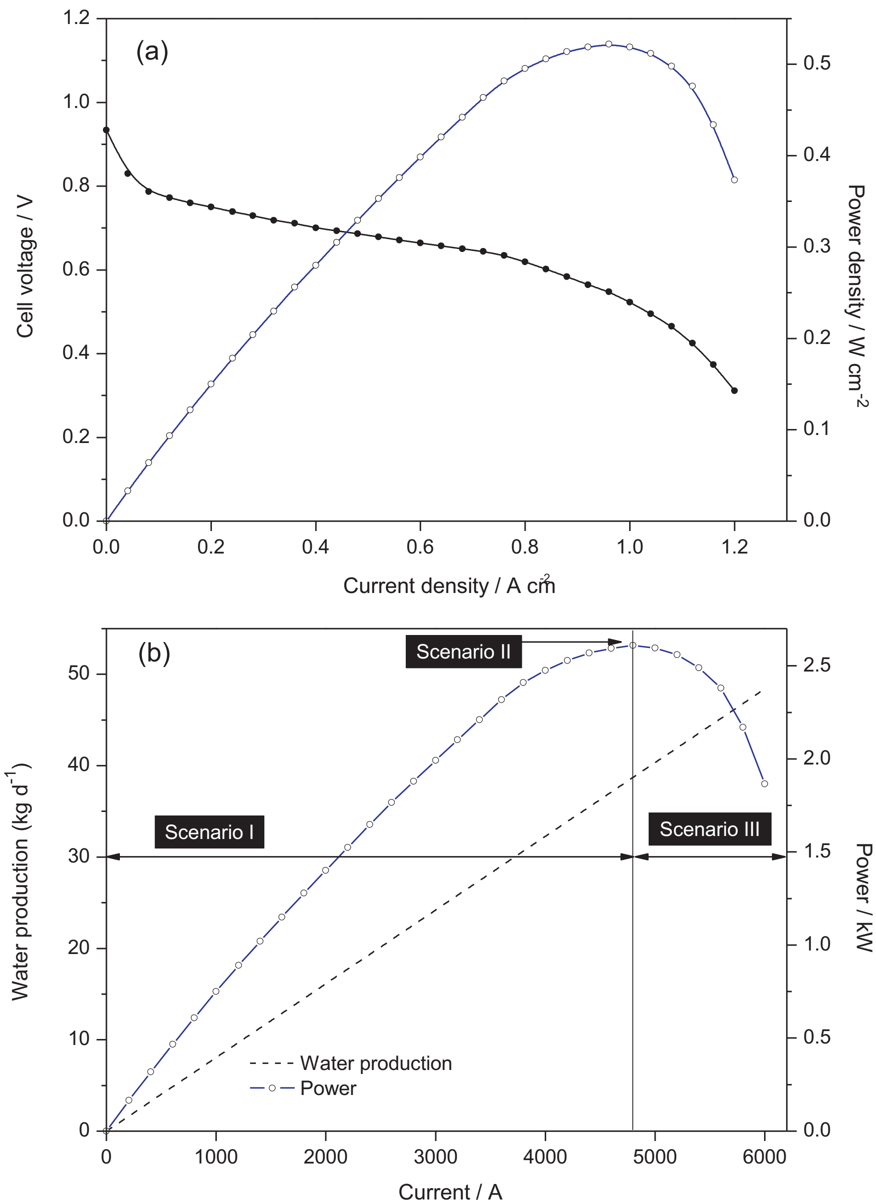


Fig. 1. (a) Polarization (filled symbols) and power density curves (open symbols) of PEM fuel cell. (b) Plot of the water production rate (dash line) and power density (open symbols). The fuel cell performance is estimated from published values of Ref. [10]. It is assumed that the number of polymer membrane and active area are 50 EA and 100 cm^{-2}, respectively.

may be related to leaching of these materials from the plumbing or from fuel cell materials. They concluded that the water collected from PEM fuel cell systems may be 'safe' as an alternative source of drinking water. These results showed that the quality of water generated by PEM fuel cells was higher than the quality of typical tap water and that the quality was in compliance with regulations that have been established by National Aeronautics and Space Administration (NASA) and the U.S. Environmental Protection Agency (U. S. EPA).

3. Scenario for water and energy production from PEM fuel cell

In a PEM fuel cell, water is produced at the rate of 1 mol for every two electrons and can be expressed by Eq. (1):

$$\text{Water production} = \frac{iAM_w}{2F} (\text{kg s}^{-1}) \quad (1)$$

where i is the current density ($A\,cm^{-2}$), A is the total area of the polymer membrane (cm^2), M_w is the molecular mass of water (18.02×10^{-3} kg mol^{-1}), and F is the Faraday constant (96,485 C mol^{-1}).

Hristovski et al. [3] showed that a commercial PEM fuel cell stack (i.e., Mark 1020 ACS) manufactured by Ballard Power Systems, Inc., which is compromised of 46 membranes with a total current of 2392 A and a power of 1.63 kW, can produce approximately 19.3 kg d^{-1} of water, assuming two-phase water capture of 100%. While this water production rate is insufficient to meet the non-internal, consumptive uses of water in a typical household (e.g., bodily contact, washing, outdoor use, and commercial activities), it is sufficient for meeting the potable water needs of a typical U.S. household [7]. Additionally, it is possible to generate sufficient potable water quantity by running the fuel cell at maximum power and increasing the number of polymer membrane.

Fig. 1(a) shows that the electrical power increases to a maximum and then decreases due to oxygen mass-transport resistance

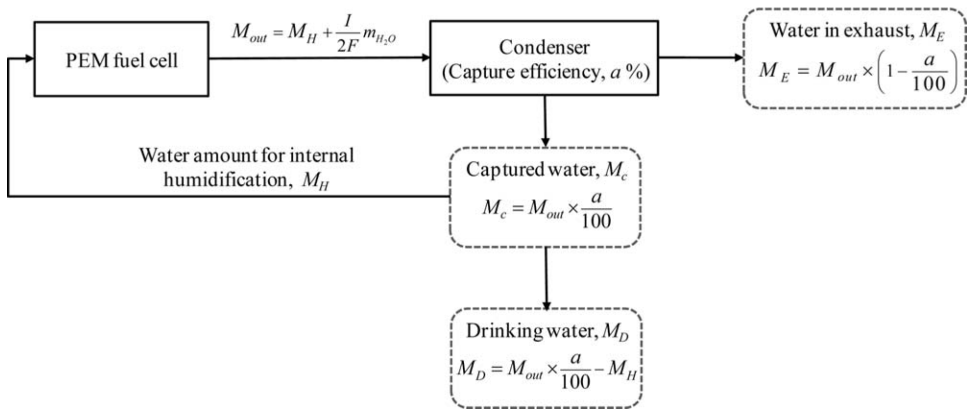


Fig. 2. Schematic of water cycle in a fuel cell with internal humidification at steady state.

by water flooding at high current. In order to increase the amount of product water from PEM fuel cell, it needs to increase the limiting current density without water flooding. Additionally, Fig. 1(b) presents that water production increases linearly with current density. These show that water and electrical power productions are classified according to electrical power produced by stack (i.e., Scenario I-stage before maximum electrical power, Scenario II-stage at maximum electrical power, and Scenario III-stage after maximum electrical power).

Scenario II and III can produce maximum electrical power and water, respectively. However, scenario III is in an unfavorable condition for production of electrical power due to severe potential drop by water flooding. A main limitation in scenario III results from the transport of reactants from the gas flow channel to the catalyst layer, referred to as the oxygen mass-transport limitation. This limitation is further amplified by the presence of liquid water, which blocks some of the open pores in the gas diffusion layer (GDL) and thus reduces the available paths for the transport of reactant species. This phenomenon, commonly referred to as water flooding, is more severe in the cathode at high current density because the slower oxygen reduction reaction is more susceptible to the negative impact caused by flooding. Thus, in point of water and energy production, Scenario II is the better than Scenario III.

In order to increase the production of water and electricity by PEM fuel cells, the limiting current density must be increased while avoiding the flooding induced by accumulated liquid water in the GDL and gas flow channel. The main limitation that prevents the achievement of high current density results from the transport of reactant gases from the gas flow channel to the catalyst layer, referred to as the oxygen mass-transport limitation. This limitation is exacerbated by the presence of liquid water, which blocks some of the open pores in the GDL and thus reduces the available paths for the transport of reactant species. Consequently, it is important to remove excessive liquid water in the GDL and gas flow channel in order to increase the limiting current density. The material and operational parameters of PEM fuel cells can effectively reduce water flooding and increase cell potential at high current density. Material parameters are generally divided into polymer electrolyte membrane, GDL, micro-porous layer (MPL), and gas flow channel designs. Operational parameters are associated with the relative humidity, reactant flow rate (i.e., gas stoichiometry), and pressure of the inlet reactant gases and the operational temperature of the cell. All of these parameters have strong impacts on the performance of the fuel cell, and they are interrelated by non-linear relationships.

In addition to increasing the limiting current density in PEM fuel cells, the provision of input water for hydration of the polymer membrane influences the amount of drinking water produced. Usually, PEM fuel cells should be fully hydrated by an external humidification system to ensure high proton conductivity, which increases the performance of the cell and its water production at the cathode. However, a PEM fuel cell that does not require external humidification of the reactant gases is highly desirable from the engineering perspective of power generation, because the extra cost of humidification equipment can exceed the savings produced by a smaller and lighter fuel cell [8]. Additionally, it is possible to eliminate the parasitic losses attributed to heating the gas humidifiers. Also, non-humidified gases are richer in fuel or oxidant per unit volume compared to the equivalent wet gas streams, which favors higher cell efficiency [9]. In attempts to overcome these problems, internal humidification by recycled exhaust gas has been used for polymer membrane hydration in PEM fuel cells, as shown in Fig. 2. However, if the input water mass (i.e., M_H) for humidification of the reactant gases increases dramatically during the cell operation, there is a sharp decrease in the amount of drinking water (i.e., M_D) generated by the PEM fuel cell because the efficiency of the condenser in capturing effluent water is not perfect. Thus, minimal use of humidification (i.e., dry or slightly humidified gas streams) for reactant gases is desirable in order to produce more drinking water without affecting electrical power productivity. However, the performance of PEM fuel cells that are operated with dry or slightly humidified gas streams is significantly decreased due to the increase of ohmic resistance compared to cells with analogous, well-humidified gas streams. Technically, the performance of a PEM fuel cell in terms of voltage and power density can be greatly influenced by various operating parameters, such as reactant gas stoichiometry, operating pressure, and cell temperature. In addition, these operational parameters can affect the relative humidity of the exit gases, which must be within a proper range for stable cell performance. Therefore, it is essential to quantify the effects of operational parameters on the performance and water production rate of PEM fuel cells.

4. Mass balance for reactant and product species in a PEM fuel cell

At steady-state conditions in a PEM fuel cell, mass balances for reactant and product species can be described by the law of conservation of mass, as depicted in Fig. 3. The mole numbers associated with each reactant and product are related to the operational conditions and are provided in Table 1. To derive the formula of mass balance, pressure drop on the cathode side and the anode side were neglected and that the water generated by the electrochemical reaction exists in the vapor phase. The relationship between the molar flux of reactant and product species and the partial pres-

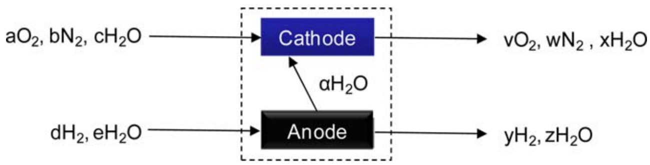


Fig. 3. Schematic diagram of the mass balance for reactant and product species in a PEM fuel cell.

Table 1
Mole numbers associated with reactant and product during PEM fuel cell operation.

	$\mathrm{mol\,s^{-1}}$
Oxygen flow rate at cathode inlet	$a = 0.21\lambda_c \frac{iA}{4F}$
Hydrogen flow rate at anode inlet	$d = \lambda_a \frac{iA}{2F}$
Nitrogen flow rate at cathode inlet and outlet	$b = w = 0.79\lambda_c \frac{iA}{4F}$
Input water supplied for cathode humidification	$c = \lambda_c \frac{RH_{c,in}p_c^{sat}}{(p_c - RH_{c,in}p_c^{sat})} \frac{iA}{4F}$
Input water supplied for anode humidification	$e = \lambda_a \frac{RH_{a,in}p_a^{sat}}{(p_a - RH_{a,in}p_a^{sat})} \frac{iA}{2F}$
Unused oxygen flow rate	$v = (0.21\lambda_c - 1)\frac{iA}{4F}$
Unused hydrogen flow rate	$y = (\lambda_a - 1)\frac{iA}{2F}$
Water content at cathode outlet	$x = \lambda_c \frac{RH_{c,in}p_c^{sat}}{(p_c - RH_{c,in}p_c^{sat})} \frac{iA}{4F} + \frac{iA}{2F} + \alpha \frac{iA}{F}$
Water content at anode outlet	$z = \lambda_a \frac{RH_{a,in}p_a^{sat}}{(p_a - RH_{a,in}p_a^{sat})} \frac{iA}{2F} - \alpha \frac{iA}{F}$

sure at the exits of the cathode and the anode, respectively, can be expressed as:

$$\frac{x}{v+w} = \frac{p_{c,w,out}}{p_c - p_{c,w,out}} = \frac{\lambda_c(RH_{c,in}p_c^{sat}/(p_c - RH_{c,in}p_c^{sat}))(iA/4F) + (iA/2F) + \alpha(iA/F)}{(\lambda_c - 1)(iA/4F)} \quad (2)$$

$$\frac{z}{y} = \frac{p_{a,w,out}}{p_a - p_{a,w,out}} = \frac{\lambda_a(RH_{a,in}p_a^{sat}/(p_a - RH_{a,in}p_a^{sat}))(iA/2F) - \alpha(iA/F)}{(\lambda_a - 1)(iA/2F)} \quad (3)$$

where $p_{c,w,out}$ and $p_{a,w,out}$ are partial pressures of the water at the cathode and anode outlets, respectively; p_c and p_a are the total pressures at the cathode and anode inlets, respectively; p_c^{sat} and p_a^{sat} are the saturated water vapor pressures at the cathode and anode inlets, respectively; λ_c and λ_a are the air and hydrogen stoichiometry numbers (i.e., ratio of the actual flow rate of reactant at the fuel cell inlet to the consumption rate of that reactant); $RH_{c,in}$ and $RH_{a,in}$ are the air and hydrogen relative humidities at the inlets, respectively; i is the current density; A is the total membrane area; F is the Faraday constant; α is the net water drag coefficient. (The net water drag coefficient, α, represents the net water molecule per proton flux ratio through the polymer membrane. When α value is less than zero, there is a net water transport towards the anode. For a detailed explanation of α, please see Ref. [10])

Thus, the relative humidity of the gases at the cathode and anode outlets are, respectively, defined as:

$$RH_{c,out} = \frac{p_{c,w,out}}{p_{cell}^{sat}} = \frac{p_c[\lambda_c(RH_{c,in}p_c^{sat}/(p_c - RH_{c,in}p_c^{sat})) + 2 + 4\alpha]}{p_{cell}^{sat}[\lambda_c(p_c/(p_c - RH_{c,in}p_c^{sat})) + 1 + 4\alpha]} \quad (4)$$

$$RH_{a,out} = \frac{p_{a,w,out}}{p_{cell}^{sat}} = \frac{p_a[\lambda_{H_2}(RH_{in,a}p_{in,a}^{sat}/(p_a - RH_{in,a}p_{in,a}^{sat})) - 2\alpha]}{p_{cell}^{sat}(\lambda_{H_2}[p_a/(p_a - RH_{in,a}p_{in,a}^{sat})] - 2\alpha - 1)} \quad (5)$$

where $RH_{c,out}$ and $RH_{a,out}$ are the relative humidities of air and hydrogen, respectively, at the outlet, and p_{cell}^{sat} is the saturated water vapor pressure at the given cell temperature.

To calculate the mass of water to be added to the air and hydrogen inlet gases to achieve a specific humidity at a given pressure and cell temperature, it must be noted that the mass of any species in a mixture is proportional to the product of the molecular mass and the partial pressure [8].

$$\frac{m_{c,w}}{m_{c,d}} = \frac{18 \times p_{c,w,in}}{28.97 \times (p_c - p_{c,w,in})} = 0.622\frac{p_{c,w,in}}{(p_c - p_{c,w,in})} = 0.622\frac{RH_{c,in}p_c^{sat}}{(p_c - RH_{c,in}p_c^{sat})} \quad (6)$$

$$\frac{m_{a,w}}{m_a} = \frac{18 \times p_{a,w,in}}{2.016 \times (p_a - p_{a,w,in})} = 8.929\frac{p_{a,w,in}}{(p_a - p_{a,w,in})} = 8.929\frac{RH_{a,in}p_a^{sat}}{(p_a - RH_{a,in}p_a^{sat})} \quad (7)$$

where $m_{c,w}$ and $m_{a,w}$ are the masses of water present in air and hydrogen gases at inlets, respectively (i.e., required input water mass for humidification); $m_{c,d}$ and $m_{a,d}$ are the masses of dry air and dry hydrogen gases, respectively; $p_{c,w,in}$ and $p_{a,w,in}$ are the partial pressures of vapor-phase water at cathode and anode inlets, respectively.

The required masses of water for inlet air humidity and inlet hydrogen humidity can be calculated from Eqs. (6) and (7), respectively, when the masses of dry air and hydrogen gases per second are expressed as Eqs. (8) and (9) at any current I of a PEM fuel cell:

$$m_{c,d} = 3.57 \times 10^{-7} \times \lambda_c \times I \quad (8)$$

$$m_{a,d} = 1.05 \times 10^{-8} \times \lambda_a \times I \quad (9)$$

As shown in Fig. 2, if a % of the effluent water from the condenser can be captured, the amount of available drinking water per day (M_D, $\mathrm{kg\,d^{-1}}$) from a PEM fuel cell with an internal humidification system can be calculated as follows:

$$M_D = M_C - M_H = \left(M_H + \frac{m_{H_2O}I}{2F}\right)\frac{a}{100} - M_H = \frac{m_{H_2O}I}{200F}a - M_H\left(\frac{100-a}{100}\right) \quad (10)$$

where M_c is the amount of captured vapor-phase water at the condenser per day; M_H is the amount of water supplied for internal humidification per day; m_{H_2O} is the molecular mass of water; and a is the capture efficiency of the effluent water from the condenser.

5. Review on parameters for increasing the amount of water source produced from PEM fuel cell

In order to get more drinking water from PEM fuel cells with internal humidification system, it is desirable to increase the limiting current density for high water production or/and reduce the amount of water feeding for humidification of reactant gases. However, PEM fuel cells operated with dry or slightly humidified gas streams for the reduction of input water show significantly decreased cell performance due to increase of ohmic resistance compared to cells with analogous well-humidified gas streams.

In this work, first, the effects of humidification of the cathode and anode on current characteristics are described for a particular configuration of a PEM fuel cell that uses an MPL only on the cathode side. This initial work is being conducted in an attempt to understand the effects the humidification of each feed stream on cell performance and to effectively reduce the amount that enters

a PEM fuel cell. Additionally, based on the overall reactions in a PEM fuel cell at steady state under the single-phase flow condition (i.e., the relative humidity of the exiting gas is less than 100%), useful guidelines for suitable ranges of operational parameters were provided. For the single-phase flow condition, the limiting current density can be increased due to the reduction of oxygen-transport resistance induced by excessive liquid-phase water accumulated in the GDL and the gas flow channel. Second, assuming that the quality water produced by the PEM fuel cell is higher than typical tap water and complies with regulations established by the U.S. EPA, the models are designed to identify the optimum operational parameters for increasing the amount of drinking water produced by PEM fuel cells.

5.1. Humidification of the inlet air and hydrogen feed streams

In general, the water inside the polymer membrane is transported mainly by electro-osmotic drag (i.e., the dragging of water molecules from the anode to the cathode by the current-carrier protons), back-diffusion (i.e., the transfer of water into the membrane due to the water concentration gradient from the cathode to the anode), and convection (i.e., water movement that occurs due to the pressure gradients between the cathode and the anode in the fuel cell). However, the convection effect is generally negligible compared to the effects of electro-osmotic drag and back diffusion. Since a PEM fuel cell is normally supplied with pure hydrogen gas and air at same pressure, the water flow due to convection can be ignored because there is no pressure difference between the anode and cathode. Thus, electro-osmotic drag and back diffusion dominate the water transport inside the polymer membrane of a PEM fuel cell.

To increase the amount of available drinking water from a PEM fuel cell, the limiting current density in a given catalyst area should be increased since the water production rate is proportional to the current. A higher current density results in greater water transport from the anode to the cathode due to electro-osmotic drag. Thus, if back diffusion of water from the cathode to the anode through the polymer membrane is insufficient to maintain sufficient water in the polymer membrane at the dry hydrogen condition (i.e., water concentration at the cathode side is very low due to insufficient humidification of the cathode), the performance of the cell may be significantly decreased due to the increase of ohmic resistance due to the low water content in the polymer membrane. These phenomena are consistent with other studies of the effects of cathode humidification on cell performance [11,12]. Yan et al. [11] tested the effect of various humidity conditions of reactant gases on cell performance with Nafion 117 (e.g., this membrane thickness is 178 μm) polymer membrane. Cell performance tests with *I–V* curves were conducted for $RH_{c,in}$ levels at the cathode of 10, 50, 70, and 100% and for $RH_{a,in}$ levels at the anode of 60, 70, 80, 90, and 100%. Their results showed that low $RH_{c,in}$ values (e.g., $RH_{c,in}$ = 30 and 50%) can exacerbate membrane dehydration by reducing back diffusion from the cathode at cell temperature of 80 °C and $\lambda_c/\lambda_a = 2/2$ conditions. Humidification of the gas at the anode helped to counteract membrane dehydration at high levels of anode humidification. They concluded that there was sufficient back diffusion with medium and high $RH_{c,in}$ values (e.g., 70 and 100%) to keep the membrane hydrated, and further humidification of the anode did not improve the performance of the cell significantly. Cai et al. [12] also compared performance and ohmic resistance at different humidity conditions using a Nafion 112 (e.g., this membrane thickness is 51 μm) membrane and a constant current density of 0.5 A cm^{-2} at cell temperature of 60 °C and $\lambda_c/\lambda_a = 2.5/1.1$ conditions. When the $RH_{a,in}$ value at the anode changed from 0 to 100% with an $RH_{c,in}$ value of 56% at the cathode, the both average outputs of the cell voltage was 0.660 V under dry and saturated hydrogen conditions and ohmic resistance slightly decreased from 0.221 Ω cm^{-2} to 0.216 Ω cm^{-2}. It was shown that, when $RH_{a,in}$ increased from 0 to 100% at $RH_{c,in}$ value of 56%, there were insignificant changes in membrane resistance and cell performance. However, when the $RH_{c,in}$ value at the cathode was changed from 56% to 36% with an $RH_{c,in}$ value of 0% at the anode, the average output of the cell voltage decreased from 0.660 V to 0.619 V and ohmic resistance slightly increased from 0.221 Ω cm^{-2} to 0.267 Ω cm^{-2}. They insisted that, when the value of $RH_{c,in}$ at the cathode was changed from 56% to 35% at dry $RH_{a,in}$ condition, back diffusion was weaker and ohmic resistance was increased significantly due to low water content in the polymer membrane. As a result, Yan et al. [11] and Cai et al. [12] concluded that the effect of cathode humidification on cell performance was more important than the effect of anode humidification.

In this work, we also evaluated the effects of the systematic dehydration of the feed streams on the performance of a PEM fuel cell using Gore-PRIMEA-18 membrane electrode assembly (MEA). The MEA consists of a membrane with a thickness of 18 μm and a catalyst layer with a thickness of 12 μm with a Pt loading of 0.4 mg cm^{-2}. The surface area of the MEA was 25 cm^2. The SGL 10BC (i.e., GDL with MPL, SGL Carbon Group, USA) and 10BA (i.e., GDL without MPL, SGL Carbon Group, USA) were used for cathode and anode GDLs, respectively. The gas flow channel used for the anode and the cathode sides were identical single-serpentine, parallel channels. The width, depth, and land width in the gas flow channel are 1 mm. The experiments described below follow a general protocol of monitoring cell current at a fixed cell potential of 0.6 V. In order to verify the effects of humidification levels of hydrogen and air feed gases on cell performance, the relative humidity of the hydrogen feed-gas stream was set to 10, 30, 50, 80, and 100% with a fully saturated air feed-gas stream at a cell temperature of 80 °C and total air pressure of 1 atm. The relative humidity of the air feed-gas stream was set to be 10, 30, 50, 80, and 100% with a fully saturated hydrogen feed-gas stream. The H_2/air stoichiometries were 1.46 and 2.5, respectively. The counter-flow mode was used. The pipes between the humidifier and the fuel cell were heated to 90 °C to avoid the condensation of water vapor.

Fig. 4(a) presents the variations of the current in the cell for a 25 cm^2 active area that is subject to various levels of $RH_{a,in}$ when there is 100% relative humidity at $RH_{c,in}$. Fig. 4(a) shows that the current levels were stable for the three segments of the cell when it was operating with $RH_{a,in}$ values of 50, 80, and 100%. However, cell performance diminished slightly as the humidification level of the hydrogen gas stream decreased (i.e., low $RH_{a,in}$ values of 10% and 30%). For instance, when slightly humidified hydrogen gas with an $RH_{a,in}$ value of 10% was fed, the average output current of the cell was approximately 21.5 A at a constant voltage of 0.6 V, for which current fluctuations were small.

However, as is shown in Fig. 4(b), the average current decreased markedly from approximately 26.3 A to 9.7 A for a cell with saturated hydrogen gas in which the $RH_{c,in}$ conditions decreased from 100% to 10% when $RH_{a,in}$ was fully humidified. As a consequence, these results also indicate that the influence of the humidification condition at the cathode on variations in output current is more significant than the influence of humidification condition at the anode. This means that the performance of the cell is affected significantly by back diffusion, which is controlled by the humidification conditions of the feed gases. Thus, if the amount of water at the cathode is increased by well-humidified air gas, the water transport by back diffusion will be enough to effectively retain the proton conductivity when the humidification at the anode is low at high current density. However, for the dry air condition, insufficient back diffusion was responsible for the dehydration of the membrane at high current density. When the air is dry, there will be a significant change in the current due to membrane dehydration. Thus,

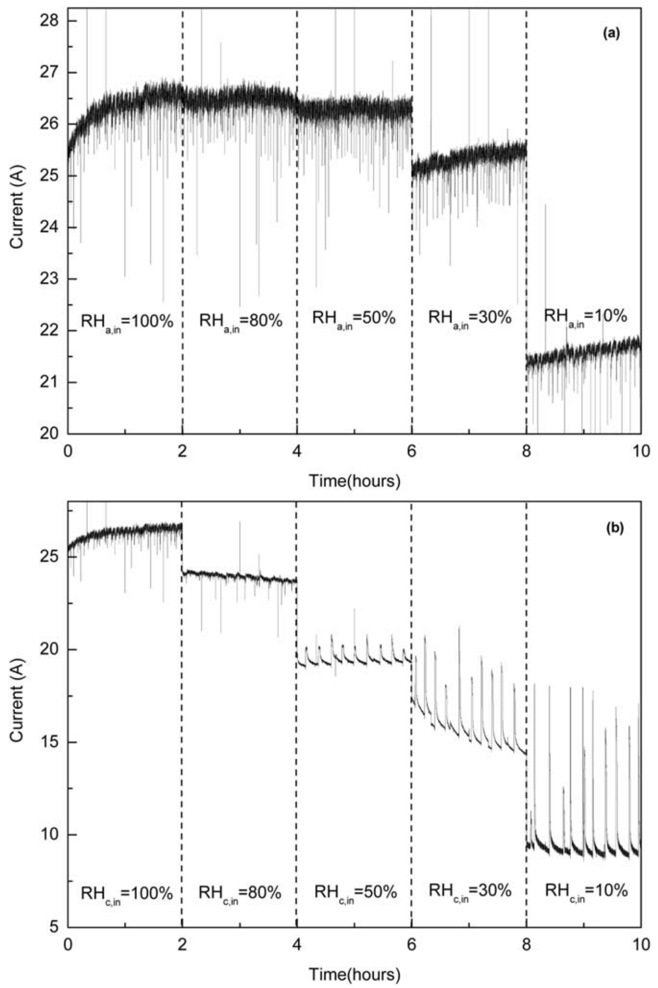


Fig. 4. Current variation as functions of time and the RH_{in} of inlet reactant gases at constant 0.6 V cell potential for a 25 cm^2 Gore-PRIMEA-18 MEA (membrane thickness of 18 μm): (a) variation of anode $RH_{a,in}$ at constant cathode $RH_{c,in}$ = 100%; (b) variation of cathode inlet $RH_{c,in}$ at constant anode inlet $RH_{a,in}$ = 100%.

when dry hydrogen gas is supplied to the fuel cell, it is important to supply well-humidified air for effective water and electrical power production at high current density.

5.2. Polymer membrane thickness and material

The thickness of the polymer membrane has a major impact on the performance of the cell and on water production at low humidification. If the value of $RH_{c,in}$ is reduced to increase the production of drinking water, the membrane thickness is a very important consideration for stable cell operation at low humidification conditions. For a thin membrane, the back diffusion of water may be sufficient to counteract the anode-drying effect due to electro-osmotic drag. However, for a thicker membrane, drying may occur on the anode side due to insufficient back diffusion of water. This was demonstrated very vividly by Büchi and Scherer [13], who created thick membranes by combining several layers of Nafion membranes. They showed that the membrane resistance is independent of current density variation for polymer membranes up to a thickness of 120 μm, but it increases for thicker membranes. Janssen and Overvelde [14] also studied the net water transport in an operating fuel cell with Nafion 105 (e.g., membrane thickness = 127 μm) and 112 (e.g., membrane thickness = 51 μm) membranes and determined the net water transport across the polymer membrane. As expected, the Nafion 112 membrane exhibited somewhat lower net water transport than the thicker Nafion 105 membrane. Values of −0.3 to +0.1 were reported when the Nafion membrane was changed from Nafion 112 to Nafion 105. (The negative values refer to the case in which back diffusion is greater than electro-osmotic drag.) Additionally, they showed that no significant dependence was found on the stoichiometry of the reactants or pressure differential, indicating that hydraulic permeation may be negligible for these membranes. Also, Cai et al. [12] indicated that, for the dry hydrogen condition, the cell with the Nafion 115 membrane (e.g., membrane thickness = 127 μm) had lower performance than the cell with the Nafion 112 membrane (e.g., membrane thickness = 51 μm) due to the increased resistance of the membrane. They suggested that a thin membrane was more proper for the operation of a fuel cell with dry hydrogen. Consequently, when a PEM fuel cell is operated to produce drinking water at a dry hydrogen condition, a thin polymer membrane and high $RH_{c,in}$ (e.g., $RH_{c,in}$ = 50–100%) can be expected to alleviate the dehydration of the membrane due to sufficient back diffusion.

The decrease of membrane thickness reduces water shortage problems in PEM due to increase of the water back-diffused from the cathode to the anode. However, this usually accelerates the crossover of H_2 and O_2 through the thin polymer membrane, which decreases the cell performance and the fuel utilization by the chemical short-circuit reaction [15]. Hence, the management of water content and reactant crossover is recognized as a key technology to enhance the cell performance and to suppress the degradation of PEM. Attempting to overcome these problems, Watanabe et al. [16–18] developed the self-humidifying PEM with highly dispersed nanometer sized Pt and/or metal oxides (i.e., TiO_2, SiO_2). The metal oxide particles that have hygroscopic property were expected to adsorb the water produced at Pt particles together with that produced at the cathode. The cells with these PEMs exhibited superior cell voltage at high current density and decreased crossover even under a dry or low-humidified condition. Gnana Kumar et al. [19] fabricated a modified Nafion membrane with silica and silica sulfuric acid for the lower humidity. Their results show that with the hydroscopic effort, high water molecules retention provokes the self humidification of modified Nafion membrane.

5.3. Stoichiometry, pressure, and temperature

The water mass balance in the polymer membrane can be described as follows. At the anode, water gain is caused by the humidified hydrogen gas and back diffusion, while water loss is caused by electro-osmosis and the evaporated water that is in the effluent gases. At the cathode, water gain is from the humidified air gas, electro-osmosis, and the water that is produced by the oxygen reduction reaction. Water is removed by back diffusion and evaporation into the unsaturated air. At both sides, these water gains and losses dominate the water distribution and water content in the polymer membrane, and they are of considerable importance in understanding the performance of PEM fuel cells.

Weber and Newman [20] established a water transport model in MEA and investigated the water distribution in MEA. They indicated that, due to electro-osmosis and water production at the cathode site, moles of water per mole of sulfonic acid at the interface of the membrane/cathode catalyst layer is higher than that at the anode site, even though the relative humidities for both the anode and the cathode are the same. Thus, if the number of moles of water per mole of sulfonic acid at the cathode site decreases due to low water gain at the cathode site, the polymer membrane at the anode site will be dehydrated dramatically due to the decreased back diffusion. As a result, the water content of the polymer membrane is primarily dominated by the water activity at the cathode site or by the relative humidity ($RH_{c,out}$) of the exit air, which is determined by total water gain and loss at the cathode. Larminie and Dicks [8]

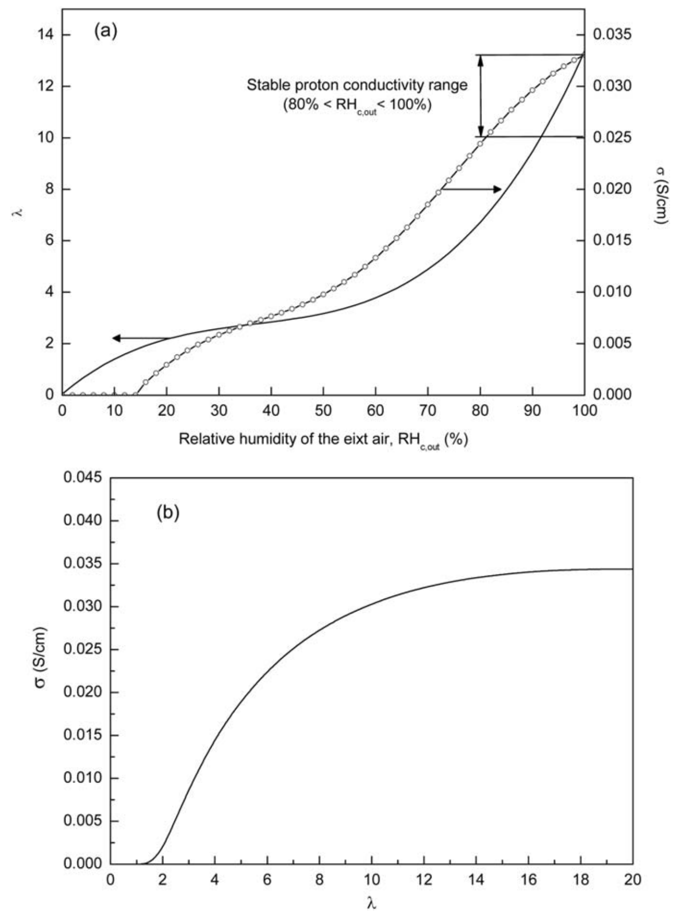


Fig. 5. (a) Variation of proton conductivity and water content equilibrated with vapor-phase water according to changes in the relative humidity of the exit air ($RH_{c,out}$), (b) relationship between the proton conductivity of a polymer membrane and its water content (*Equivalent weight (EW)* of polymer membrane = 950).

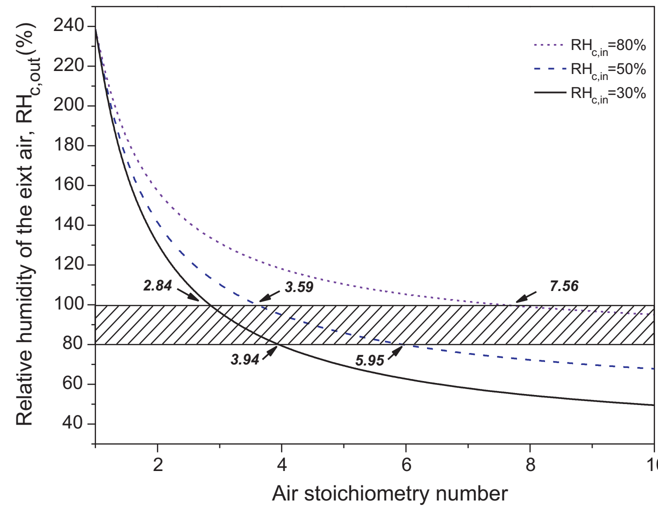


Fig. 6. Relative humidity of the exit air stream *vs*. air stoichiometry number for various relative humidities at the cathode inlet with a total air pressure of 1.1 atm.

more clearly suggested that the suitable range of $RH_{c,out}$ for stable cell operation should be above 80% to prevent membrane dehydration, but it must be less than 100% to avoid water flooding in the GDL, electrode, and gas flow channel.

Thampan et al. [21] proposed a proton conductivity (σ) model in polymer membranes as a function of the water content (λ). (For more detailed information about the proton conductivity model, please see Ref. [21]) Using the aforementioned proton conductivity model, we represent the variation of proton conductivity and water content equilibrated with vapor-phase water according to the change of $RH_{c,out}$, as shown in Fig. 5(a). It can be seen that proton conductivity decreases rapidly as the $RH_{c,out}$ decreases below 80%. Using the suitable range of $RH_{c,out}$ from 80 to 100% for stable cell operation, a proton conductivity is presented in Fig. 5(a) under suitable $RH_{c,out}$ range (i.e., $\lambda > 10$ and $\sigma = 0.025–0.333\ \mathrm{S\,cm^{-1}}$). In addition, we represent the relationship between the proton conductivity of the polymer membrane and its water content at a cell temperature of 80 °C as shown in Fig. 5(b). It can be seen that, when the water content is less than 2, the polymer membrane behaves like an insulator. Above this threshold, the proton conductivity of the membrane increases significantly as the water content in the polymer membrane increases. When the water content is greater than 10, the proton conductivity of the membrane reaches a plateau. As shown in Fig. 4(a), this means that the PEM fuel cell can be stably operated in the range of proper water content (i.e., $\lambda > 10$ when $RH_{c,out}$ is in the suitable range of 80–100%). As mentioned earlier, the operational parameters (i.e., $RH_{c,in}$, air stoichiometry, total air pressure, and cell temperature) have strong impacts on the suitable range of $RH_{c,out}$ and are related among themselves by non-linear relationships. Eq. (4) can be used to analyze the influences of the various operational parameters on $RH_{c,out}$.

Fig. 6 shows the relationship between air stoichiometry and $RH_{c,out}$ under various $RH_{c,in}$ conditions at a given cell temperature of 80 °C. Based on previous experimental results from a study by Kim et al. [10], in which the MPL was only on the cathode, the net water drag coefficient was assumed to be $\alpha = -0.27$. It can be seen in Fig. 6 that $RH_{c,out}$ decreases significantly as the air flow rate increases at a given $RH_{c,in}$. Additionally, the curves of proper range of $RH_{c,out}$ *vs*. air stoichiometry number are presented in the shaded zone of Fig. 5, according to the suggestion of Larminie and Dicks [8]. This indicates that, when the curves of proper $RH_{c,out}$ *vs*. air stoichiometry number fall in the shaded zone, the PEM fuel cell can be operated stably. Above the shaded zone, vapor-phase water would condense in the cell components, causing water flooding at the cathode side. Below the shaded zone, it would be difficult to keep the membrane hydrated.

In general, the air stoichiometry (λ_c) is normally determined in the range of 2–4, which is dependent on the operational condition of the fuel cell and material design. A lower air stoichiometry (e.g., $\lambda_c < 2$) will cause poor cell operation due to the reduction of the concentration of available oxygen, which results in increased concentration over-potential, whereas a higher air stoichiometry (e.g., $\lambda_c > 4$) will result in the reduction of oxygen utilization as well as the rapid evaporation of water due to rapid flow of oxygen gas. Therefore, under various $RH_{c,in}$ conditions, the appropriate air stoichiometry range should be determined for better cell performance, as shown in Fig. 6. For the case in which $RH_{c,in}$ = 80%, the appropriate air stoichiometry range is too high to operate under these operation conditions. If the air stoichiometry range for $RH_{c,in}$ = 80% is from 2 to 4, water condensation in the fuel cell may impair the operation of the cell due to the resistance to oxygen transport caused by the hindrance of liquid water at a lower stoichiometry number. In addition, although air stoichiometry at $RH_{c,in}$ = 30% is within the optimal range, low $RH_{c,in}$ values of 10% and 30% are expected to affect the performance of the cell adversely, as shown in Fig. 4(b). This may be limited primarily due to low proton conductivity. Furthermore, a dry air environment can also slow down the charge transfer process. Zhang et al. [22] showed that, with dry reactant gases, the resistance to charge transfer is 1.5–2.0 times higher than the resistance when the reactant gases are fully saturated. This could be due to the reduction of the Pt surface area in the dry catalyst layers. Even though the oxygen and hydrogen concentrations were high

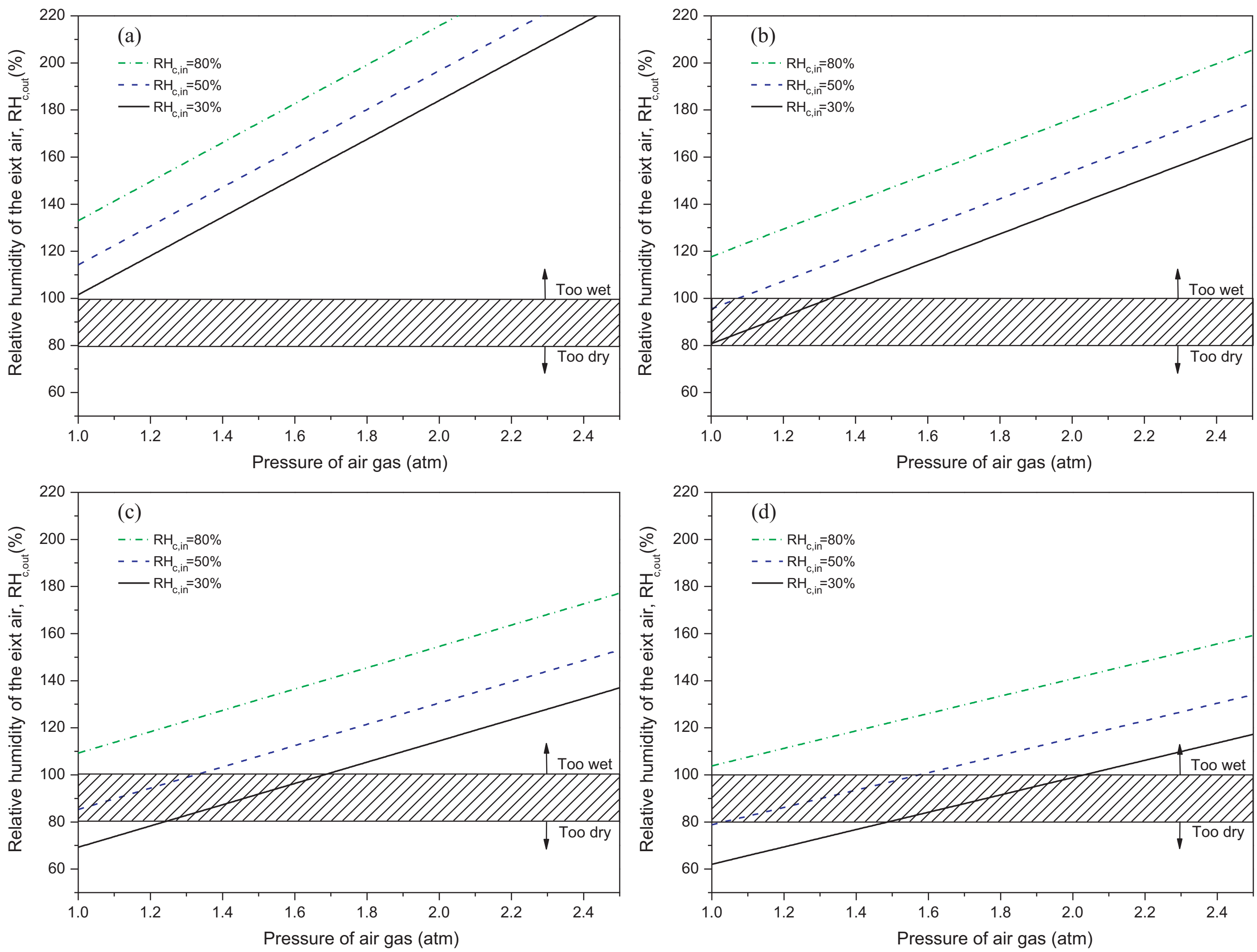


Fig. 7. Calculated relative humidity of the exit air stream as a function of air pressure at different air stoichiometry numbers: λ_c = (a) 2.5, (b) 3.5, (c) 4.5, and (d) 5.5. Common physical parameters: net water drag coefficient of −0.27 and cell temperature of 80 °C.

due to high gas stoichiometry, a large resistance to mass transfer occurred at dry or slightly humidified reactant gas conditions due to the limited proton transfer process to Pt catalysts. This was observed mainly in dry ionomer medium within a dry electrode, and it occurred in addition to the increase in charge transfer resistance at dry or slightly humidified air conditions. Consequently, it is important to determine the proper air stoichiometry range of 2–4 considering the aspect of $RH_{c,in}$ = 50% for the reductions of various resistances as well as the amount of inlet water amount supplied for air humidification. If the $RH_{c,in}$ condition is less than 50%, the total air pressure should be increased to keep the membrane hydrated at low humidity conditions at the cathode.

Fig. 7 presents a further evaluation of the relationship between $RH_{c,out}$ and total air pressure at various air stoichiometry numbers. It can be seen that $RH_{c,out}$ is proportional to the total air pressure. When the saturation partial pressure of water vapor is only a function of cell temperature and the cell temperature is constant during cell operation, the mole fraction of water vapor in the exhaust air gas is determined primarily by total air pressure. This is because, as the total air pressure becomes higher, the mole fraction of water vapor in the exhaust air gas would decrease (i.e., $x_{H_2O} = P^{sat}/P_c$). Thus, the amount of water leaving with the exhaust air gas becomes lower, and the number of moles of water in the fuel cell increases. This results in the increase of the vapor pressure of the water in the fuel cell. This leads to the important conclusion that a system with higher air pressure requires less added water to achieve the same humidity of exit air and increases the amount of drinking water produced by the PEM fuel cell due to the reduction of amount of water used for the humidification of reactant gases.

Furthermore, cell operation at higher air pressure increases cell performance due to various causes. Zhang et al. [22] showed that cell performance increases significantly with increasing gas pressure at dry reactant gas conditions due to the increase of the partial pressure of the reactant gases and the reduction of the volumetric flow rate of the reactant gases. These factors lead to increases in the amounts of water retained in both the cathode and the anode. Additionally, the increased pressure raises the exchange current density, which has the apparent effect of increasing the open circuit voltage (OCV). In addition to these benefits, there is also a reduction in the mass transport losses due to the increase in the partial pressure of oxygen in the catalyst layer [11]. However, additional power is consumed to increase the air pressure when a fuel cell must be operated at higher air pressure. Thus, voltage gains and losses associated with increasing the air pressure should be considered. Consequently, the pros and cons of adding the extra air compressor apparatus must be considered. These problems will be discussed later.

Additionally, there is usually a strong relationship between the cell temperature and water production rate in a fuel cell, since cell temperature has a major impact on relative humidity (RH). The RH is defined as the ratio of the partial pressure of water to the saturated vapor pressure of water at a given temperature. The saturated vapor

Table 2
Input water mass rate in appropriate range of air stoichiometry at different $RH_{c,in}$ conditions.

$RH_{c,in}$ (%)	λ_c	M_H (kg d^{-1})	Input water/product water
30	2.84–3.94	18.8–26.0	0.97–1.35
50	3.59–5.95	43.7–72.4	2.26–3.75
80	7.56–	175<	9.07<

pressure increases more and more rapidly above 60 °C. This means that, when the partial pressure of vapor water is constant, $RH_{c,in}$ decreases to a significant extent as the internal temperature of the fuel cell exceeds 60 °C. This is because the pressure of the saturated water vapor must increase significantly to achieve the same relative humidity in the inlet stream to the cathode if the temperature is above 60 °C. Thus, the input water mass rate for the appropriate cathode humidification increases more and more rapidly above 60 °C, which results in decrease of the amount of available drinking water from PEM fuel cell with internal humidification.

6. Drinking water production rate from PEM fuel cell

The mass of water to be added to the air stream depends to a great extent on operational parameters such as $RH_{c,in}$, air stoichiometry, total air pressure, and cell temperature. Therefore, another objective of the present work is to conduct technical quantification and assessment of the effect of operational parameters on input water mass rate (i.e., M_H, kg d^{-1}) for air humidification and on the drinking water production rate (i.e., M_D, kg d^{-1}) of the PEM fuel cell. To calculate the amount of water production (i.e., M_P, kg d^{-1}) generated by the oxidation-reduction reaction at the cathode, it is assumed that a PEM fuel cell stack is operated with a total current of 2392 A (i.e., 52 A per polymer membrane and 46 membranes in a fuel cell stack [23] and can produce approximately 19 kg of water per day. As mentioned earlier, this water production rate from commercial fuel cell stack can be increased by the improvement of the current density as well as increase of the number of polymer membrane. However, we only focus on increase of available drinking water from PEM fuel cell by reduction of water feeding for humidification of reactant gases.

Assuming that no humidification at the anode (dry H_2), Fig. 8 shows the M_H for cathode humidification and ratio of input water to water produced as function of air stoichiometry at different $RH_{c,in}$ conditions at a total air pressure of 1.1 atm. As one would expect, Fig. 8 indicates that the M_H is proportional to the air stoichiometry. Furthermore, the M_H increases significantly as $RH_{c,in}$ increases. Table 2 shows the ratio of input water to product water (i.e., M_H/M_P) and the M_H values within the appropriate range of air stoichiometry values in Fig. 6 at different $RH_{c,in}$ conditions. Except for low air stoichiometry at $RH_{c,in}$ = 30%, the M_H/M_P is always greater than 1 at $RH_{c,in}$ = 50% and 80%. This means that, if the capture efficiency at the condenser is not 100%, the product water generated by the electrochemical reaction at the cathode will be consumed for humidifying the cathode. This leads to a sharp reduction of M_D whereas M_H increases significantly. Thus, other operational parameters should be considered to reduce M_H for humidification of the cathode. Fig. 9 indicates the reduction of M_H for humidification of the cathode as total air pressure increases at different $RH_{c,in}$ conditions. For instance, it can be seen that, at an air pressure of 1.5 atm, the M_H/M_P is less than 1, except for $RH_{c,in}$ = 80%. However, the M_H for humidification of the cathode is not greatly reduced until the air pressure is 3 atm.

As mentioned earlier, running a fuel cell at higher pressure will increase the electrical power due to reductions in the cathode activation overvoltage as well as oxygen-transport loss. However,

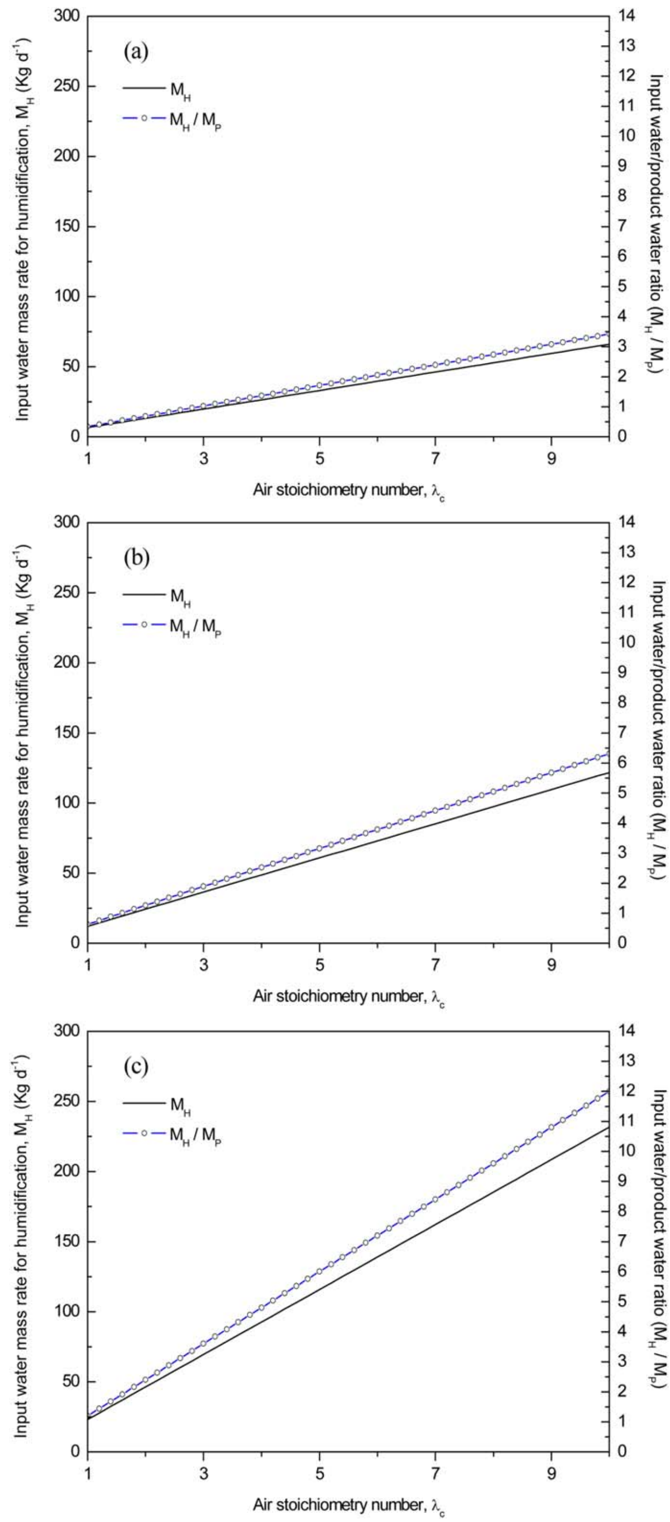


Fig. 8. Calculated input water mass rate (M_H) for cathode humidification and input water/product water ratio (M_H/M_P) as a function of air stoichiometry number at different $RH_{c,in}$ conditions: $RH_{c,in}$ = (a) 30%, (b) 50% and (c) 80%. Common operational parameters: cell temperature of 80 °C and total air pressure of 1.1 atm.

operating the fuel cell at higher pressure involves the expenditure of parasitic power taken up by the compression equipment. To consider the pros and cons of increasing the air pressure, the voltage loss and gain, as well as the increase of M_D at higher total air pressure, must be considered more quantitatively. The voltage gain and loss are changed according to the increase of the operational pres-

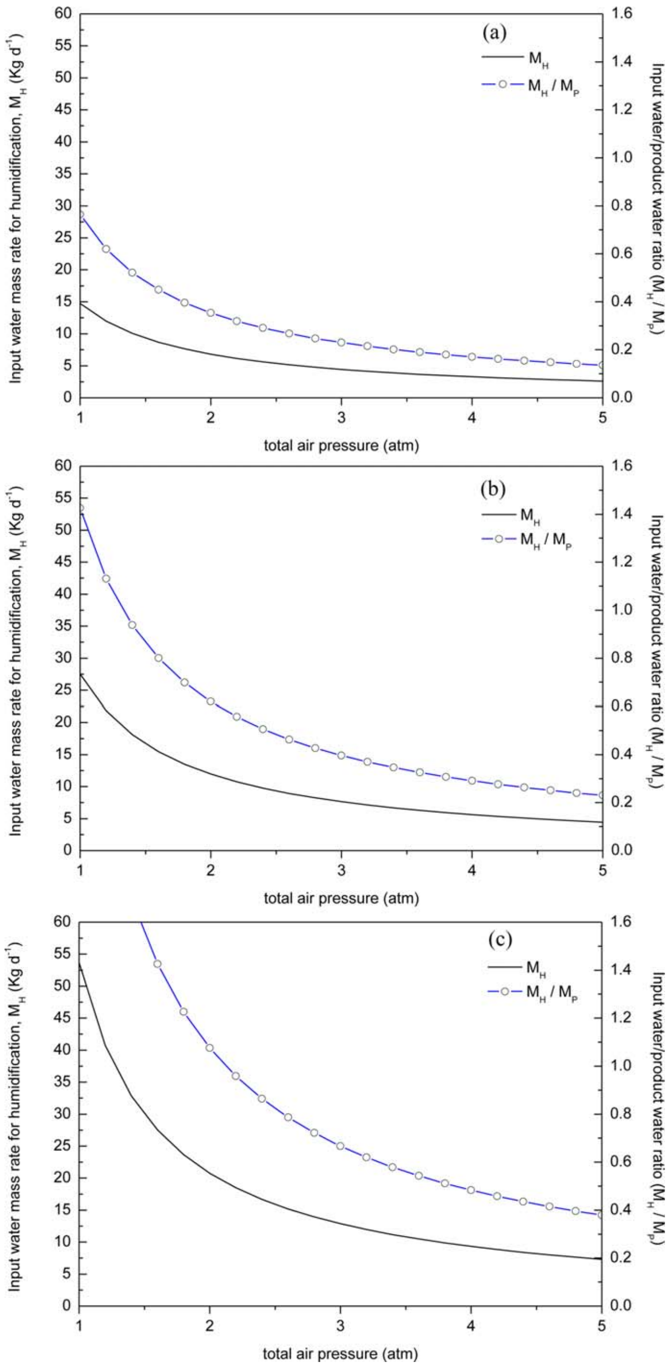


Fig. 9. Calculated input water mass rate (M_H) for cathode humidification and input water/product water ratio (M_H/M_P) as a function of air pressure at different relative humidity of cathode inlet: $RH_{c,in}$ = (a) 30%, (b) 50% and (c) 80%. Common operational parameters: cell temperature of 80 °C, air stoichiometry of 2, total current of 2392 A.

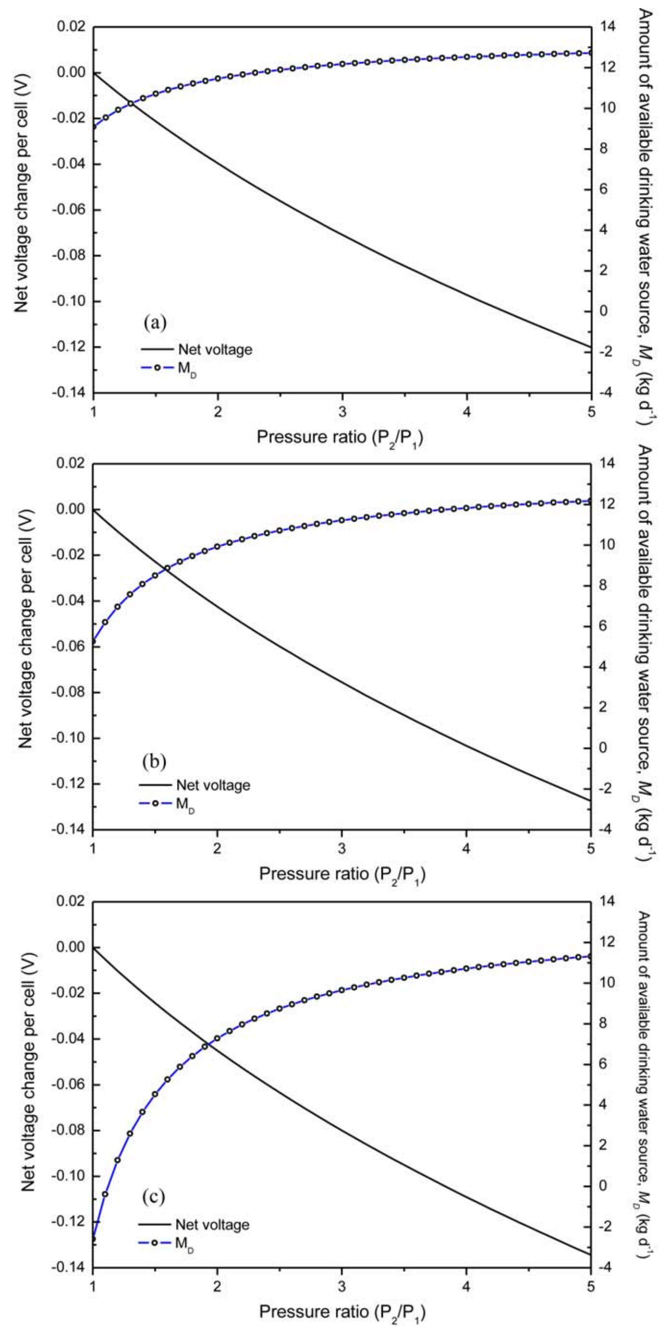


Fig. 10. Net voltage change and amount of available drinking water (M_D) resulting from initial ambient air pressure (1 atm) and higher pressures: $RH_{c,in}$ = (a) 30%, (b) 50% and (c) 80%. Common operational parameters: cell temperature of 80 °C, air stoichiometry of 2, total current of 2392 A. The capture efficiency, *a*, is assumed to be approximately 70%. Actually, Chu and Jiang [26] were able to capture only approximately 66% of the theoretical amount of effluent water under STP conditions due to evaporation and other losses.

sure from an original value of P_1 to a higher pressure P_2. The net voltage change resulting from operating at higher pressure can be calculated as follows [8]:

$$Net\Delta V = \Delta V_{gain} - \Delta V_{loss} = C\ \ln\left(\frac{P_2}{P_1}\right) - 3.58\times 10^{-4} \times \frac{T_1}{\eta_c\eta_m}\left(\left(\frac{P_2}{P_1}\right)^{0.286} - 1\right)\lambda_c \quad (11)$$

where *C* is a constant the value of which depends on how the exchange current density is affected by pressure and temperature. It is not clear what value should be used for *C*. Parsons, Inc. has reported figures ranging from 0.03 to 0.06 V [24]. Hirschenhofer et al. [25] used a constant value of 0.06 V. In this work, we used 0.06 V as a constant value. The last term on the right side of Eq. (11) can be written for the voltage loss by the compressor in terms of compressor efficiency η_c (η_c = 0.7) [8], the efficiency of the electric drive for the compressor η_m (η_m = 0.9) [8], and the entry temperature of the air stream, T_1.

Eqs. (10) and (11) were used to plot the graph of net voltage change and M_D at different $RH_{c,in}$ conditions, as shown in Fig. 10. The data presented in Fig. 10 show that there is always a net voltage

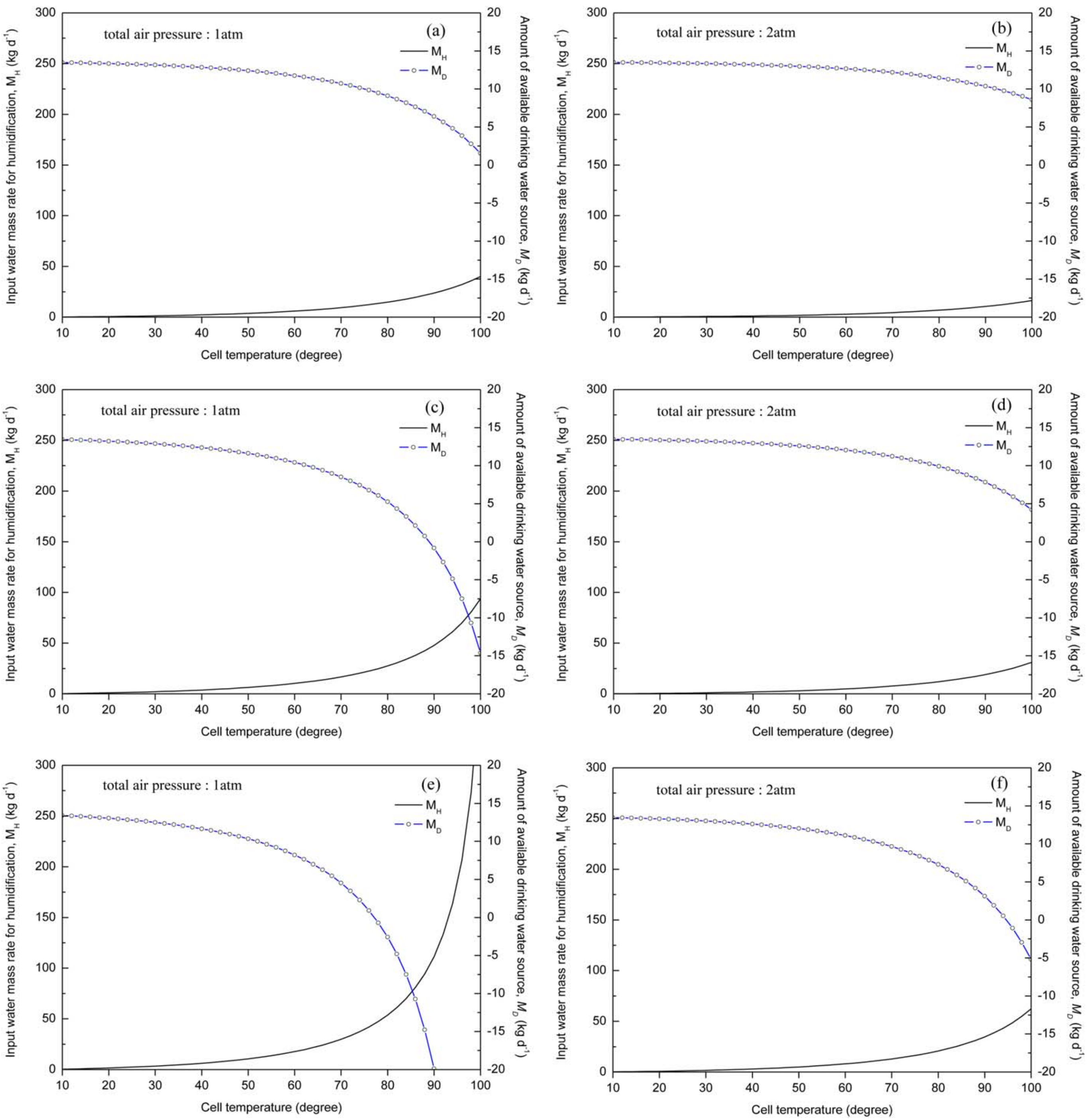


Fig. 11. Input water mass rate for humidification (M_H) and amount of available drinking water (M_D) as a function of cell temperature at different total air pressure and $RH_{c,in}$ conditions: (a) and (b) $RH_{c,in}$ = 30%, (c) and (d) $RH_{c,in}$ = 50%, (e) and (f) $RH_{c,in}$ = 80%. Common physical properties: capture efficiency of 70%, total current of 2392 A, and air stoichiometry of 2.

loss as a result of the higher pressure. This means that the additional electrical power needed to drive the compressor is always exceeded by the power gained. Furthermore, it can be expected that a higher net voltage loss at a higher cell temperature and air stoichiometry will be observed due to the greater voltage losses associated with air compression, which result in a larger ΔV_{loss}, as given by Eq. (11). For this reason, the practice of operating above atmosphere pressure is by no means universal, even with larger PEM fuel cells. With smaller fuel cells, i.e., less than about 5 kW, are rare, since the compressors are likely to be less efficient and more expensive [8]. However, this pressurization process is needed to provide sufficient drinking water for a household, as shown in Fig. 10. With higher $RH_{c,in}$, the M_D will increase as the total air pressure increases since the amount of water required at the cathode inlet to achieve the same humidity will be less at higher pressure. Therefore, at high $RH_{c,in}$, it is recommended that the fuel cell be operated at the higher pressure of 3 atm to achieve a greater water production rate. For an $RH_{c,in}$ value of 30%, however, the pressurization process does not materially affect the production of drinking water from the PEM fuel cell.

As mention earlier, the cell temperature above 60 °C significantly affects the amount of feeding water for the humidification

of reactant gases. This results in a sharp increase of M_H for cathode humidification at cell temperatures above 60 °C. It can be seen from Fig. 11(a) that, at a total air pressure of 1 atm, M_D is always greater than zero over the full range of cell temperatures from 10 to 100 °C. In Fig. 11(c) and (e), however, it can be seen that, at temperatures above 60 °C, M_D decreases very markedly during the internal humidification process. Thus, in order to produce M_D values greater than 10 kg d^{-1} at different $RH_{c,in}$ conditions, it is desirable to maintain the temperature of the fuel cell at less than 60 °C. At low cell temperatures, small amounts of water are needed to saturate the air, and M_D is more than sufficient. However, a low cell temperature results in lower cell potential. This is because lower cell temperature results in exponentially lower exchange current density and significantly hinders the oxygen-mass transport properties at the cathode side, whereas increased cell temperatures can increase the kinetics of both oxygen reduction and hydrogen oxidation reactions. However, increased cell temperatures can accelerate the evaporation of water evaporation at low $RH_{c,in}$ values, resulting in a reduction of water retention in the polymer membrane and an increase in ohmic resistance. This has a negative effect on the performance of the cell. Furthermore, if more M_H should be supplied to a PEM fuel cell in order to maintain proper proton conductivity at high cell temperature, the high cell temperature significantly decreases the M_D. Thus, the M_D, as well as a trade-off between water retention in the polymer membrane and reaction kinetics, should be considered. Zhang et al. [22] studied the effect of 23 °C and 60 °C cell temperatures on cell performance with dry reactant gases. They showed that, at low current density (i.e., <0.3 A cm^{-2}), the cell performances at both cell temperatures were almost the same, with a higher performance relative to high current density at 60 °C. This indicates that water retention in the polymer membrane was higher at 23 °C than at 60 °C, but the reaction rates were slower at 23 °C than at 60 °C. The trade-off between water retention and reaction kinetics may be responsible for the similar cell performances for low current densities less than 0.3 A cm^{-2}. At higher current densities, however, the positive impact of increased reaction kinetics at 60 °C on the cell performance may overwhelm the negative impact of less water retention and result in higher cell performance.

As a result, at low current density with low cell temperature, it is possible to maintain the cell's electrical and water production performances. However, at high current density, the amount of drinking water available will be significantly decreased to maintain the same $RH_{c,in}$, even though the cell's electrical performance is higher than it is at low cell temperature. In order to reduce the amount of water that must be added to humidify the reactant gases at high cell temperature as well as to maintain high current density, increasing the air pressure is more effective, as shown in Fig. 11(b), (d), and (f). It can be seen that, even though the $RH_{c,in}$ condition and the cell temperature increase, the M_D at a total air pressure of 2 atm is greater than that at ambient pressure.

7. Conclusions

In this work, useful guidelines were developed along with their respective operational parameters for maintaining stable performance of the cell and for increasing the amount of drinking water produced by the PEM fuel cell. These guidelines were based on the overall reaction in a PEM fuel cell at steady state. As the results indicate, the minimal use of humidification (i.e., dry or slightly humidified gas streams) is desirable for significantly increasing the amount of drinking water from the PEM fuel cell without affecting electrical power productivity by low humidification. However, when a PEM fuel cell operates with dry or low-humidity gases, the result is significantly decreased cell performance due to increased ohmic resistance. Specifically, the influence of the humidification condition at the cathode on current variation was more important than the influence of the humidification condition at the anode. Thus, for stable cell performance, the humidity of the air at the outlet ($RH_{c,out}$) should be above 80% to prevent membrane dehydration, but it must be kept less than 100% to avoid flooding the PEM fuel cell with water. The proper $RH_{c,out}$ is dependent to a significant extent on operational parameters, such as air inlet humidification ($RH_{c,in}$), air stoichiometry, air pressure, and operating cell temperature. When the inlet gas humidity at the anode is very low (dry gas) and air stoichiometry is in the normal range of 2–4, the appropriate $RH_{c,in}$ is 50% to ensure sufficient water content in the polymer membrane and stable cell performance. If $RH_{c,in}$ is less than 50%, air pressure should be increased to maintain sufficient water content in the polymer membrane. This is important because the mole fraction of water vapor in the exhaust air decreases as total air pressure increases. In addition, cell operation at high air pressure will increase the performance of the cell due to the reduction of cathode activation overvoltage. However, when a fuel cell must be operated at higher air pressure, additional power is consumed to increase the air pressure. Thus, voltage gains and losses associated with increasing the air pressure should be considered. There is always a net voltage loss when air pressure increases, but the pressurization process is required to provide sufficient drinking water (i.e., >10 kg d^{-1}) for a household. For the low $RH_{c,in}$ condition, the pressurization process does not materially affect the amount of drinking water produced by a PEM fuel cell. However, for a high $RH_{c,in}$ condition, the mass of the input water is decreased significantly as air pressure increases. However, the water required for humidification at a high $RH_{c,in}$ condition is not greatly reduced for an air pressure greater than 3 atm. Furthermore, it is clear that, above a cell temperature of 60 °C, the amount of available drinking water decreases markedly, since saturated water vapor pressure increases more and more rapidly above this temperature, which means that the partial pressure of dry air and the $RH_{c,out}$ both decrease significantly. Consequently, in order to produce more than 10 kg d^{-1} of drinking water at different $RH_{c,in}$ conditions, it is desirable to decrease the operating cell temperature to less than 60 °C. The water production rate from a PEM fuel cell is dependent on limiting current density and the number of polymer membrane. In general, at limiting current density, the water yield from PEM fuel cells would not be sufficient to meet the internal consumptive uses of water in typical households. Thus, an increase in the number of polymer membrane at low current density is an alternative solution for increasing the amount of drinking water from a PEM fuel cell.

Acknowledgement

This research has been performed as Project No. WI08STU06 and was supported by the Korea Water Resources Corporation (K-Water).

References

[1] Narayan GP, Sharqawy MH, Summers EK, Lienhard JH, Zubair SM, Antar MA. The potential of solar-driven humidification–dehumidification desalination for small-scale decentralized water production. Renewable and Sustainable Energy Reviews 2010;14:1187–201.

[2] U.S. Geological Survey 2008. Residential energy consumption survey. Available at: http://ga.water.usgs.gov/edu/wupt.html/.

[3] Hristovski KD, Dhanasekaran B, Tibaquirá JE, Posner JD, Westerhoff PK. Producing drinking water from hydrogen fuel cells. Journal of Water Supply: Research and Technology – AQUA 2009;58(5):327–35.

[4] Sauer RL, Calley DJ. Biomedical results of Apollo-Potable water supply. Rep. No. LC-75-600030; NASA-SP-368. Houston, TX: Johnson Space Center; 1975. Available at: http://lsda.jsc.nasa.gov/books/apollo/S6CH4.htm.

[5] Collier A, Wang H, Yuan XZ, Zhang J, Wilkinson D. Degradation of polymer electrolyte membranes. International Journal of Hydrogen Energy 2006;31(13):1838–54.

[6] Orta D, Mudgett PD, Ding L, Drybread M, Schultz JR, Sauer RL. Analysis of water from the space shuttle and Mir space station by ion chromatography and capillary electrophoresis. Journal of Chromatography A 1998;804: 295–304.
[7] Aquacraft, Inc. Residential end uses of water. American Water Works Association Research Foundation; 1999. Available at: http://www.aquacraft.com/Publications/resident.htm (retrieved February 18, 2010).
[8] Larminie J, Dicks A. Fuel cell systems explained. 2nd ed. John Wiley & Sons, Ltd.; 2003.
[9] Atkins JR, Savett SC, Creager SE. Large-scale current fluctuations in PEM fuel cells operating with reduced feed stream humidification. Journal of Power Sources 2004;128:201–7.
[10] Kim T, Lee S, Park H. A study of water transport as a function of the microporous layer arrangement in PEMFCs. International Journal of Hydrogen Energy 2010;35:8631–43.
[11] Yan Q, Toghiani H, Wu J. Investigation of water transport through membrane in a PEM fuel cell by water balance experiments. Journal of Power Sources 2006;158:316–25.
[12] Cai Y, Hu J, Ma H, Yi B, Zhang H. Effect of water transport properties on a PEM fuel cell operation with dry hydrogen. Electrochimica Acta 2006;51: 6361–6.
[13] Büchi FN, Scherer GG. Investigation of the transversal water profile in Nafion membranes in polymer electrolyte fuel cells. Journal of the Electrochemical Society 2001;148(3):A181–8.
[14] Janssen GJM, Overvelde MLJ. Water transport in the proton-exchange-membrane fuel cell: measurements of the effective drag coefficient. Journal of Power Sources 2001;101:117–25.
[15] Hagihara H, Uchida H, Watanabe M. Preparation of highly dispersed SiO_2 and Pt particles in Nafion® 112 for self-humidifying electrolyte membranes in fuel cells. Electrochimica Acta 2006;51:3979–85.
[16] Watanabe M, Uchida H, Seki Y, Emori M, Stonehart P. Self-humidifying polymer electrolyte membrane for fuel cells. Journal of the Electrochemical Society 1996;143:3847–52.
[17] Watanabe M, Uchida H, Emori M. Polymer electrolyte membranes Incorporated with nanometer-size particles of Pt and/or metal-oxides: experimental analysis of the self-humidification and suppression of gas-crossover in fuel cells. The Journal of Physical Chemistry 1998;102(17):3129–37.
[18] Watanabe M, Uchida H, Emori HM. Analyses of self-humidification and suppression of gas crossover in Pt-dispersed polymer electrolyte membranes for fuel cells. Journal of the Electrochemical Society 1998;145(4):1137–41.
[19] Gnana Kumar G, Kim AR, Nahm KS, Elizabeth R. Nafion membranes modified with silica sulfuric acid for the elevated temperature and lower humidity operation of PEMFC. International Journal of Hydrogen Energy 2009;34(24):9788–94.
[20] Weber AZ, Newman J. Transport in polymer-electrolyte membrane III Model validation in a simple fuel-cell model. Journal of the Electrochemical Society 2004;151:A326–39.
[21] Thampan T, Malhotra S, Tang H, Datta R. Modeling of conductive transport in proton-exchange membranes for fuel cells. Journal of the Electrochemical Society 2000;147(9):3242–50.
[22] Zhang J, Tang Y, Song C, Cheng X, Zhang J, Wang H. PEM fuel cells operated at 0% relative humidity in the temperature range of 23–120 °C. Electrochimica Acta 2007;52:5095–101 (2007).
[23] Ballard Power Systems, Inc. Available at: http://www.ballard.com/Stationary_Power/Backup_Power_Fuel_Cells/Product_Specifications.htm.
[24] Parsons Inc, EG&G Services. Fuel cells: a handbook. 5th ed. U.S. Department of Energy; 2000. p. 3–10.
[25] Hirschenhofer JH, Stauffer DB, Engelman RR. Fuel Cells: A Handbook, Revision 3, Business and Technology Books; 1995.
[26] Chu D, Jiang R. Comparative studies of polymer electrolyte membrane fuel cell stack and single cell. Journal of Power Sources 1999;80:226–34.